Computation of the Longitudinal Dispersion Coefficient in an Adsorbing Porous Medium Using Homogenization

Aiske Rijnks[1], Mohamed Darwish[2], and Hans Bruining*[,3]
[1]StatoilHydro ASA, [2]Shell Exploration & Production International Centre, [3]TU Delft
*Corresponding author: Section of Geoengineering, Faculty of Civil Engineering and Geosciences, TU Delft, Stevinweg 1, 2628 CN Delft, The Netherlands, Email: J. Bruining@tudelft.nl

Abstract: In a pioneering paper Bouddour, Auriault and Mhamdi-Alaoui derive upscaled expressions for the dispersion coefficients for reactive flow in a porous medium using the method of homogenization. The method uses a periodic unit cell (PUC), which consists for instance of a spherical grain in a cube, but nothing prohibits defining more complex PUC's. Homogenization leads to a coupled system of equations where the flow is described by Stokes equation and the concentration fluctuation is described by a convection diffusion source term equation. In the PUC we have semi-periodic boundary conditions (BC's). The solution of the equation is not trivial due to the source term and the BC's. The same equation arises in other upscaling techniques for upscaled dispersion coefficients, such as solving equations in periodic media or REV averaging. We show that commercial finite element software (COMSOL) can be readily used to compute longitudinal and transversal dispersion coefficients in 2-D and 3-D; this makes homogenization accessible to the engineering practice. Details of the complete numerical procedure are discussed in detail. The results are for the first time compared with experimental data of the dispersion coefficient versus Peclet number; there is good agreement. Adsorption enhances the longitudinal dispersion coefficient.

Keywords: homogenization, dispersion tensor, adsorption

Introduction

Reactive transport in porous media plays an important role in environmental hydrology, petroleum engineering and agricultural engineering. Our interest was triggered by the Arsenic remediation process for drinking water in Bangladesh; if Fe^{2+} is deposited on the sand grains it shields the As adsorbing Fe^{III} oxides and hence leads to arsenic production in the drinking water wells [6]. Our interest is in upscaling from the pore-scale to the core scale (macroscopic dispersion) for the interpretation of laboratory experiments. The dispersion term is implemented in the upscaled equation by replacing the molecular diffusion by a dispersion tensor $\mathbf{D}$, which is the sum of the isotropic-tortuosity corrected molecular diffusion tensor $D_m\mathbf{I}$ and the hydrodymamic dispersion tensor $\mathbf{D_d}$.

A relatively new upscaling method [11], called homogenization, has the advantage with respect to other upscaling techniques that it does not need a closure relation for the structure of the transport terms [3] [13] [8] [5]. Reference [5] gives a more complete version of this paper. Homogenization shares with Representative Elementary Volume (REV) averaging a precise formulation involving the order of magnitude of the characteristic dimensionless numbers [17]. Tardif d'Hamonville et al. [15] was the first to develop a 3-D finite element code to solve the equations derived in [3] numerically to find values of all the components of the dispersion tensor as a function of the Peclet number. We compute the longitudinal dispersion (sum of hydrodynamic dispersion and tortuosity corrected molecular diffusion), for a wider range of Peclet numbers. For this we use commercial finite element software (COMSOL), but also other programs (e.g., FENICS) can be used. We give an overview of the idea behind homogenization in 1, and mention the derived model equations in Section 2. Section 3 deals with the numerical implementation. Section 4 makes a comparison between homogenization data and laboratory experiments reported in the literature. We end with some conclusions.

1 Procedure for homogenization

Consider a system of macroscopic (global scale) dimensions with a characteristic length L. The macroscopic domain consists of a collection of periodic unit cells, on the microscopic (local) scale with characteristic length l. To ensure the separation of scales we need that $\varepsilon = l/L << 1$. For reasons of illustration we use a simple periodic unit cell (PUC) (see Fig. 1). Inside the PUC fluid flows according to Stokes law, using periodic boundary conditions and using that the flow tangential and normal to the grain surface Γ is zero.

The transport equations are non-dimensionalized on inspection [14], where we split all spatial differentiation into a contribution on the local scale and on the global scale. In this procedure L is the characteristic length for global differentiation and l is the characteristic length for local differentiation. We obtain an equation with the usual dimensionless numbers, e.g., the Peclet number and ε. The magnitude of the Peclet number with respect to ε will be determined. Then we expand the dependent variables into contributions of decreasing significance with respect to ε. After substitution the transport equations will consist of a sum of terms each with a different order with respect to ε. Each of the terms with a specific order in ε constitutes an equation that is separately satisfied. From this the expressions for the upscaled parameters, e.g., the dispersion coefficient are obtained.

1.1 Stokes equation

We assume that the flow in the "void" space is governed by Stokes equation, which can be straightforwardly solved numerically to obtain $\mathbf{v} = \mathbf{v}(\mathbf{r}_s)$. As a result we find in each periodic unit cell the same velocity distribution, because in each PUC the flow is subjected to the same potential gradient. The velocity does not change on the global scale. Only local velocity variations, i.e., within the PUC are relevant. It is convenient to separate the divergence ∇ into a global ∇_b and a local ∇_s contribution. We notice that $\nabla_b \cdot \mathbf{v} = 0$ because of the periodicity assumption and hence we obtain from the incompressibility condition $\nabla \cdot \mathbf{v} = \nabla_b \cdot \mathbf{v} + \nabla_s \cdot \mathbf{v} = 0$

$$\nabla_b \cdot \mathbf{v} = 0, \text{ and } \nabla_s \cdot \mathbf{v} = 0 \tag{1}$$

1.2 Solute transport

The convection diffusion equation inside the PUC i.e. in Ω_l can be written as

$$\frac{\partial c}{\partial t} + \mathbf{div}\ (\mathbf{v}c) = \mathbf{div}\ (D\ \mathbf{grad}\ c) \tag{2}$$

where c is the molar Fe^{2+} concentration, $\mathbf{v}$ the velocity field obtained from the solution of the Stokes equation and D is the molecular diffusion coefficient.

The boundary condition at the grain surface in the absence of adsorption is written as

$$(-D\ \mathbf{grad}\ c)_n = \mathbf{v} = 0 \quad \text{at } \Gamma \tag{3}$$

Periodic boundary conditions are used at the boundaries of the PUC.

2 Upscaled equations

The procedure of homogenization leads to an expression of the dispersion coefficients as follows

$$\mathbf{D}_d = -\frac{D_0 Pe}{\varphi} \frac{1}{|\Omega|} \int\limits_{\Omega_l} \mathbf{v} \otimes \chi \, d\mathbf{r}_s \tag{4}$$

and

$$\mathbf{D}_m = \frac{D_0}{\varphi} \left(\varphi \mathbf{I} + \frac{\varphi}{|\Omega_l|} \int\limits_{\Omega_l} \mathbf{grad}_s \otimes \chi \, d\mathbf{r}_s \right) \tag{5}$$

where $\mathbf{v}$ is the dimensionless velocity field and te inner product of χ with the global concentration gradient $\mathbf{grad}\ c_0$ is the concentration fluctuation in the unit cell. We use the notation for the dyadic product $\mathbf{v} \otimes \chi$ in which each component of one vector multiplied by another component of the other vector forms a matrix.

For the x-component of χ we can derive the source, convection diffusion equation

$$\begin{aligned} -\frac{\bar{v}_x}{R} + \mathbf{div}_s\ (\mathbf{v}(\chi_x + x_s)) \\ = \quad \frac{1}{Pe} \mathbf{div}_s\ \mathbf{grad}_s (\chi_x + x_s) \ . \end{aligned} \tag{6}$$

with boundary conditions

$$\frac{1}{Pe} \left(\mathbf{grad}_s\ (\chi_x + x_s) \right) \cdot \mathbf{n} = 0 \text{ at } \Gamma \ , \tag{7}$$

where x_s is the x-coordinate in the unit cell. The concentration fluctuation χ_x is periodic in the unit cell. Equations for the other components of χ can be derived like-wise.

3 Numerical calculation of the dispersion coefficient

In order to calculate the full dimensional hydrodynamic longitudinal dispersion and effective diffusion coefficients we need to compute the first order concentration correction χ_x (χ_y). We solve the problem, i.e., the Stokes equation and Eq. (6) in 3-D using a Finite Element Method software package. COMSOL also allows to compute the volume integrals in Eqs. (4), (5).

For reasons of easy comparison with reference [15] we have defined the geometry in Fig. 1 for the PUC in 3-D. In each of the eight corners of the cube, spheres, representing the grains, with radii of 0.583 or 0.510 have been drawn corresponding to porosities of 0.242 and 0.446 respectively. The parts of the sphere that fall outside the unit cube are discarded, whereas the parts inside the cube constitute the grains. The overlapping parts of the spheres inside the cube belong to the porous skeleton.

We apply semi-periodic boundary conditions, i.e., periodic boundary conditions for the faces that are not perpendicular to the flow direction and semi-periodic boundary conditions for the faces perpendicular to flow. Semi-periodic boundary conditions means that, e.g., the concentration at one face is equal to the corresponding concentration at the other face augmented with the global concentration difference, which we take to be equal to one across the PUC. The same procedure is applied for the pressure, but here also the velocities are strictly periodic. The pressure difference was chosen such that the average dimensionless longitudinal interstitial velocity $\overline{v}_x$ is equal to $1/\varphi$. In the periodic unit cell consisting of the unit cube ($\xi = 1$), we take the Peclet number as $Pe = v_x\xi/D_0$, i.e. the inverse of the diffusion coefficient times the porosity $D_0\varphi$. In the literature [2] the Peclet number is usually defined as $\overline{v}d_p/D_0$, where the interstitial velocity $\overline{v} = \overline{u}/\varphi$ and d_p is the grain diameter. For our choice of inscribed radii ($a = 0.51$ or $a = 0.583$) this only leads to a minor difference.

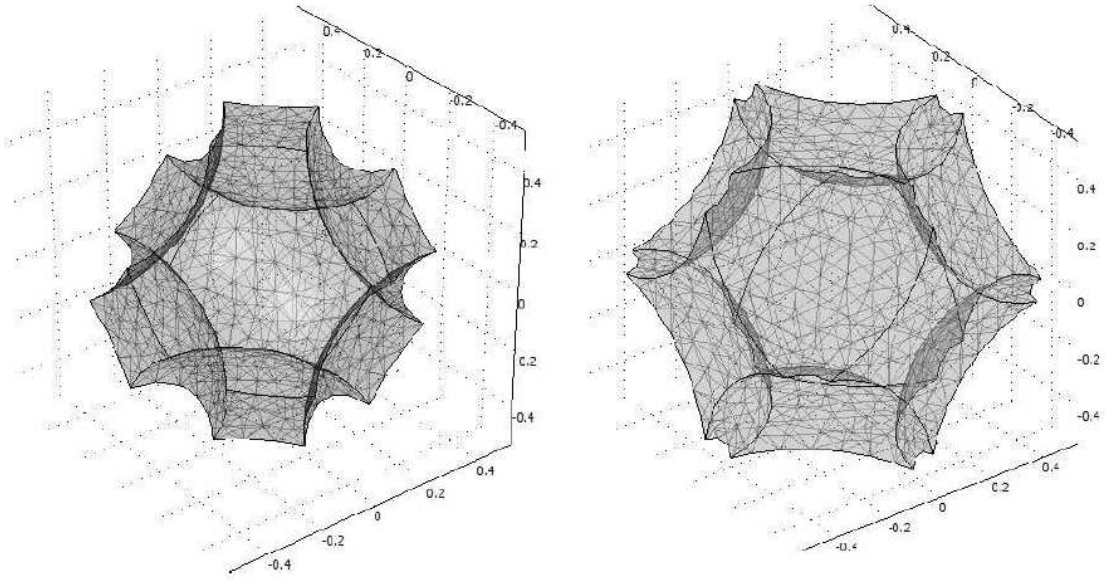

Figure 1: Part of the periodic unit cell (cube) filled with fluids left (a): Coarse Finite Element mesh with radius of spheres at te corner $a = 0.583$ and right (b): finite element mesh for $a = 0.510$ The average x-velocity is equal to $1/\varphi$.

It turns out to be advantageous to use the diffusion equation in the transient mode: $\partial c/\partial t + \mathbf{v} \cdot \ \mathbf{grad}\ c = \mathbf{div}\,(D\ \mathbf{grad}\ c) + \bar{v}_x$, where we use $c = \chi_x + x_s$ for the longitudinal coefficients. Various values of $D = \frac{1}{Pe}$ are used. For long times the solution converges to the solution of the stationary reaction-diffusion-convection equation.

To implement semi-periodic boundary conditions for the concentration equation in COMSOL, it appears to be necessary to choose the appropriate Neumann precondition at the inflow and outflow boundary; in this case we implement the Convective Flux condition $(-D\ \mathbf{grad}\ c) \cdot \mathbf{n} = 0$ to ensure that the diffusive flux or the concentration gradient is also periodic. COMSOL can solve the Stokes equation as well as the convection diffusion equation in their conservative form. A Multigrid preconditioner presolves the linear set of equations before COMSOL applies the Generalized Minimal Residual Method (GMRES).

4 Results

For the 2-D example we use a simple square array of cylinders, i.e., the PUC is a circle in a square such that the porosity $\varphi = 0.37$. Fig. 2 also compares with experimental [2] and numerical data cited in Table IV of [9]. The comparisons involve the dispersion in a 2-D periodic medium of circles inside squares for a case with porosity $\varphi = 0.37$. At the smallest resolution we used 250 triangular elements and at the highest resolution we used 4000 triangular elements, with no significant change in the results. Edwards et al. [9] used 400 nine node elements. As it turns out Edwards solves exactly the same cell equation (6), but state that they derive subsequently the dispersion coefficient from an equation derived by Brenner [4] (based on a moment analysis)%

$$\mathbf{D}_m + \mathbf{D_d} = \frac{1}{\varphi|\Omega|} \int_{\Omega_l} \nabla\chi \otimes \nabla\chi \; d\mathbf{r}_s. \qquad (8)$$

The result of using the xx component of Eq. (8) is shown in Fig. 2 as the thin drawn line below the other data. It only gives good results for very small Peclet numbers. However, the values in Table IV of [9] are exactly reproduced for low Peclet numbers if we use (the xx component) in Eq. (4) and Eq. (5) instead of Eq. (8). Buyuktas and Wallender [7] also use Eq. (6) and Eq. (4) and Eq. (5) to obtain the dispersion coefficient in the same way as in this paper. The data from Eidsath [10] also quoted in Edwards [9] disagree both with our calculations and the data of Edwards. However, Eidsath used a 36 element mesh. At higher Peclet numbers, the computed data by Edwards are higher than the experimental data and our computed results. We are not able to find a reason for this discrepancy.

Fig. 3 shows the 3-D results. The 3-D simulation with the corner spheres of radii $a = 0.510$ (0.583) was carried out with 5832 (3128) mesh points, with 27420 (14495) tetrahedal Lagrangian quadratic elements. COMSOL uses shlag(2,'c') shape functions with integration order 4 and constraint order 2. A simulation with 1731 (955) mesh points and 7746 (4068) elements gave results that deviated at most 0.133% (0.288%). At low Peclet numbers the longtudinal coefficient is dominated by the molecular diffusion. For the configuration in Fig. 1a (1b) D/D_o assumes values of 0.51 (0.69) . The measured value is $D \sim 0.7D_0$, is only attained for the configuration shown in Fig 1b. This configuration has a porosity value $\varphi = 0.446$, close to many laboratory tests ($\varphi = 0.35 - 0.45$) . The computed results show the same trends as the experimental results collected for instance in [2]. However, a similar calculation for the transverse dispersion coefficients (not displayed here) shows that the computed values are much too low.

Numerical calculations that include adsorption of solute to the grain (see Fig. 4) show in a 2-D example that adsorption (retardation $R = 10$) enhances the longitudinal dispersion coefficient, but leaves the transverse dispersion coefficient unchanged. Van Duijn et al. [16] find a similar result. In agreement with [1] we find an increasing dispersion coefficient for increasing retardation. Indeed for a Freundlich isotherm, the highest retardation and hence the largest dispersion coefficient occur at low concentrations .

The discussion is finalized with a few words about the practical relevance of the results in this paper. The first important aspect is that homogenization shows whether the proposed upscaled equation derived in this paper can be used for the interpretation of laboratory results. The main condition is that the Peclet

number on the PUC scale is of the order of unity. For iron ions with molecular diffusion coefficients in water of the order of 10^{-9} [m^2/s] this is clearly the case. For microbes with a much lower diffusion coefficient such an assumption is not correct and this has a consequence for the upscaled convection-diffusion equation for microbes. The second application is that it is in principle possible to derive the transport coefficients. The shortcoming of this clearly manifests itself in the underestimate of the transverse dispersion coefficient. Whether this problem can be circumvented by defining more complex PUC's [9] is still an open research question. As to the transport coefficients an important result is that absorption enhances longitudinal dispersion, For the time being, however, the enhancement effect appears to be too small to be of practical significance. Finally, macroscopic (pore-scale) dispersion cannot be disregarded in describing gigascopic dispersion, because it consists of a reversible and irreversible contribution [12]. The irreversible contribution is also determined by pore-scale mixing. A challenge for future work is to investigate whether homogenization can be used to come to a partition between reversible and irreversible dispersion.

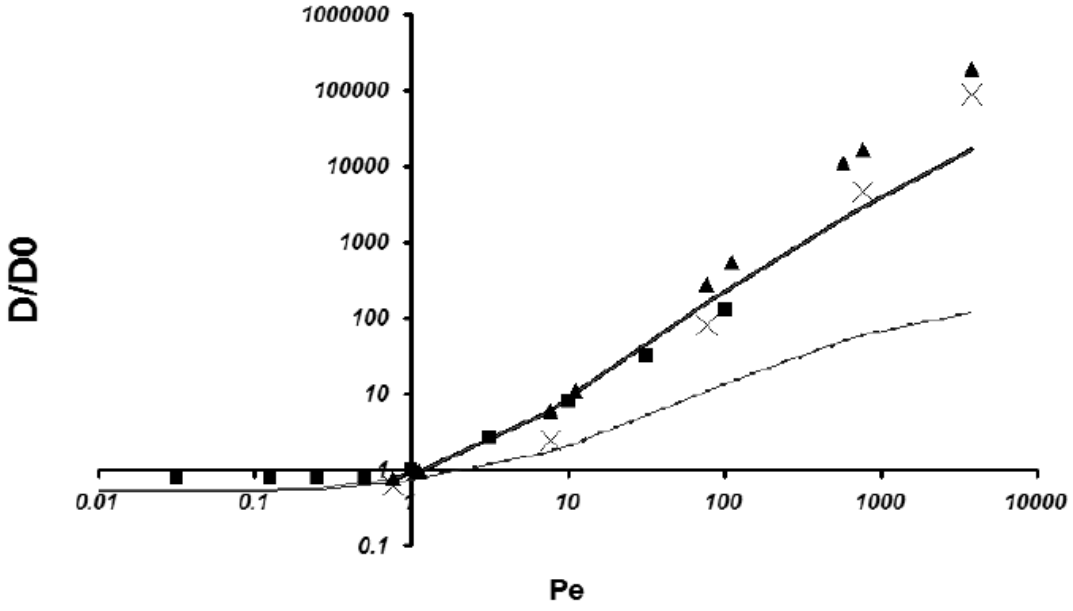

Figure 2: Comparison of the computed hydrodynamic dispersion coefficients (drawn line) for a 2D model with experimental and numerical data of other authors. The squares are the experimental data [2], the crosses are the data from [10] whereas the triangles are data from Edwards et al. [9]. The drawn curve is computed in this work for a simple square arrays of cylinders with $\varphi = 0.37$. The thin drawn line below the other data uses the cell average of $< c_x c_x >$ to estimate the dispersion coefficient.

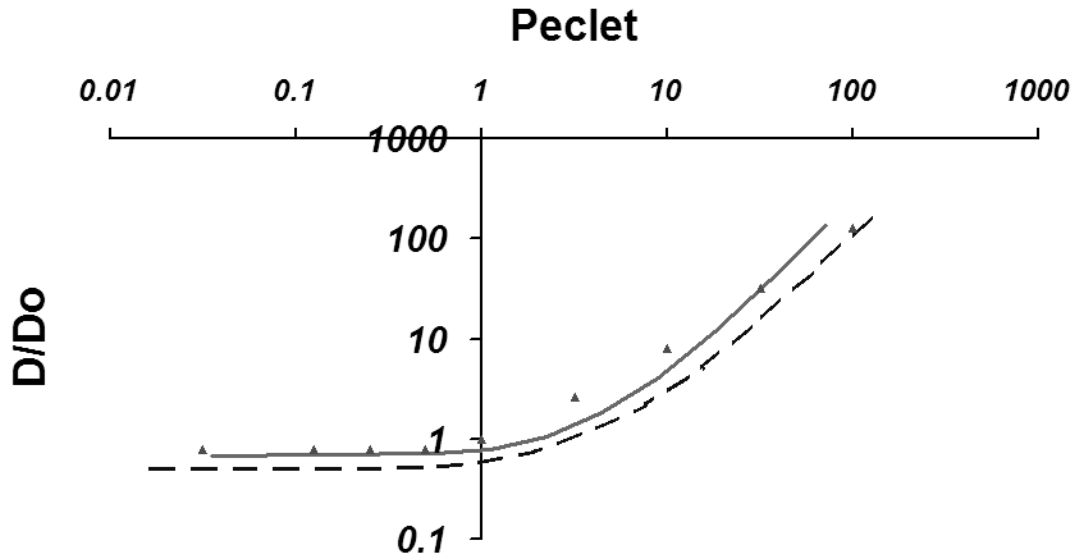

Figure 3: Longtudinal dispersion divided by molecular diffusion versus Peclet number. The Peclet number is based on the interstitial velocity $v = u/\varphi$. The characteristic dimension is the size of the unit cell. Dashed (dashed-dot-dot) line has unit cell as Fig. 1a (left) and the drawn (dashed-dot) line as Fig. 1b (right). The triangles denote experimental points [2]

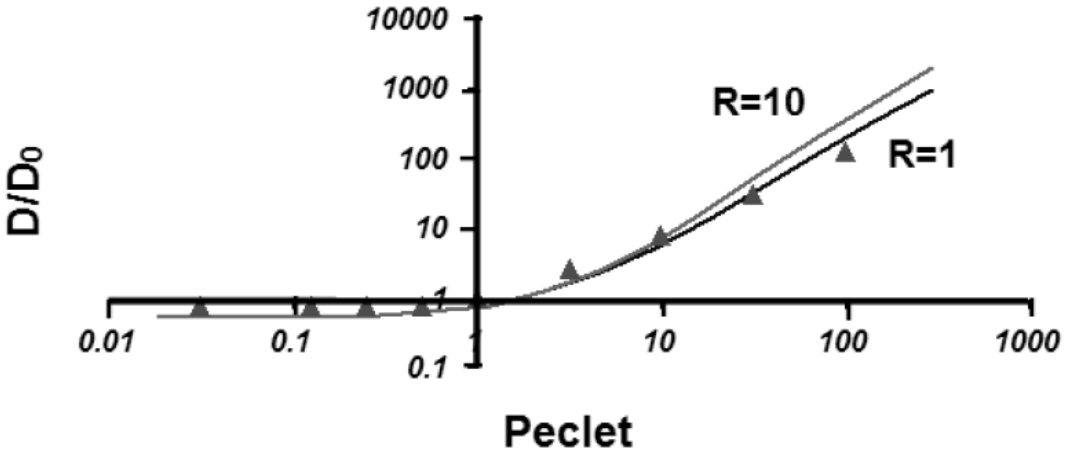

Figure 4: The effect of adsorption on the dispersion coefficient. With adsorption, i.e., the retardation factor $R = 10$, the longitudinal dispersion coefficient is higher.

Conclusions

Homogenization is a useful method to obtain upscaled equations. The method leads to upscaled equations for the laboratory scale that are less dependent on intuition than upscaled equations obtained with REV averaging.

Explicit expressions for the dispersion tensor are obtained, based on comparison to the convective diffusion equation used for contaminant transport. Commercial Finite Element Method software, e.g., COMSOL can be used to solve the unconventional equations, the solution of which is necessary to obtain 4 quantitative results.

The computed longitudinal dispersion coefficients as a function of the Peclet number show good agreement with experimental literature data.

References

[1] S. Attinger, J. Dimitrova, and W. Kinzelbach, *Homogenization of the transport behavior of nonlinearly adsorbing pollutants in physically and chemically heterogeneous aquifers*, Advances in Water Resources **32** (2009), no. 5, 767–777.

[2] J. Bear, *Dynamics of fluids in porous media*, Dover Publications, Inc., Dover, 1972.

[3] A. Bouddour, J. L. Auriault, and M. MhamdiAlaoui, *Erosion and deposition of solid particles in porous media: Homogenization analysis of a formation damage*, Transport in Porous Media **25** (1996), no. 2, 121–146.

[4] H. Brenner, *Dispersion resulting from flow through spatially periodic porous media*, Philosophical Transactions of the Royal Society of London. Series A, Mathematical and Physical Sciences **297** (1980), no. 1430, 81.

[5] J. Bruining, M. I. M. Darwish, and A. Rijnks, *Computation of the longitudinal and transverse dispersion coefficient in an adsorbing porous medium using homogenization*, Transport in Porous Media **submitted** (2009).

[6] J. Bruining and M.I.M. Darwish, *Homogenizeation for Fe^{2+} deposition near drink water tube wells during arsenic remediation*, European Conference on the Mathematics of Oil Recovery X, Amsterdam, P **3** (2006).

[7] D. Buyuktas and W.W. Wallender, *Dispersion in spatially periodic porous media*, Heat and Mass Transfer **40** (2004), no. 3, 261–270.

[8] M.I.M. Darwish and J. Bruining, *Upscaling of iron adsorption during arsenic remediation using homogenization*, 5th international congress on environmental geotechnics, Cardiff, Wales, UK (2005).

[9] D. A. Edwards, M. Shapiro, H. Brenner, and M. Shapira, *Dispersion of inert solutes in spatially periodic, 2-dimensional model porous-media*, Transport in Porous Media **6** (1991), no. 4, 337–358.

[10] A. Eidsath, S. Whitaker, R.G. Carbonell, and L.R. Herrmann, *Dispersion in pulsed systems. Pt. 3: comparison between theory and experiments for packed beds*, Chemical Engineering Science **38** (1983), no. 11, 1803–16.

[11] U. Hornung, *Homogenization and Porous Media*, Springer, 1997.

[12] John A.K. Bryant S.L. Lake L.W. Jha, R.K., *Flow reversal and mixing*, SPE Journal **March** (2009), 41–49.

[13] A. Mikelic and C. Rosier, *Modeling solute transport through unsaturated porous media using homogenization I*, Computational & Applied Mathematics **23** (2004), 195–211.

[14] M. Shook, D. Li, and L.W. Lake, *Scaling immiscible flow through permeable media by inspectional analysis*, In Situ **16** (1992), no. 4, 311–349.

[15] P. Tardif dHamonville, A. Ern, and L. Dormieux, *Finite element evaluation of diffusion and dispersion tensors in periodic porous media with advection*, Computational Geosciences **11** (2007), no. 1, 43–58.

[16] C. J. Van Duijn, A. Mikelic, I. S. Pop, and C. Rosier, *Effective dispersion equations for reactive flows with dominant peclet and damkohler numbers*, Advances in Chemical Engineering **34** (2008), 1–45.

[17] B.D. Wood, *The role of scaling laws in upscaling*, Advances in Water Resources **32** (2009), no. 5, 723–736.

Acknowledgments

The work described here was supported by The Netherlands Organisation for Scientific Research (NWO) for the project "Solubility/mobility of arsenic under changing redox conditions" (2001-2004).